IEEE Access
Multidisciplinary | Rapid Review | Open Access Journal

Received October 4, 2019, accepted November 9, 2019, date of publication December 3, 2019, date of current version December 17, 2019.

Digital Object Identifier 10.1109/ACCESS.2019.2957405

Influence of Moist Environment on Aging Performance of Energized Silicone Rubber Used for Outdoor Insulation

YONG ZHU, (Member, IEEE), SHENG XU, AND YANLIN LI
Department of Electrical Engineering, Taizhou University, Taizhou 225300, China

Corresponding author: Yong Zhu (zhuyong@tzu.edu.cn)

This work was supported in part by the Natural Science Foundation of the Jiangsu Higher Education Institutions of China under Grant 16KJB470015, and in part by the Scientific Research Foundation of Taizhou University of China under Grant QD2016053.

ABSTRACT The influence of moist environments on the aging performance of silicone rubber (SR) used for outdoor insulation was investigated by a salt-fog test. High-temperature vulcanized (HTV) SRs with different alumina trihydrate (ATH) filler contents were adopted as the test specimens. For the test of a single water droplet, the vibration and elongation of the water droplet caused a flashover, and the flashover voltage decreased with increasing ATH content. In the first cycle of the salt-fog test, the leakage current increased with increasing ATH content. The relatively higher hydrophobicity of the specimen with a low ATH content than the specimen with a high ATH content had an inhibitory effect on the initial leakage current development. In the last cycle of the salt-fog test, the heat from dry band arc discharge became the dominant factor affecting the surface aging after the loss of hydrophobicity, and the specimen with a higher ATH content inversely had a better inhibitory effect on leakage current development. According to the X-ray photoelectron spectroscopy (XPS) analysis results, when the energized SR was exposed to a moist environment, the heat from dry band arc discharge and the hydrolysis reaction caused a change in the binding state between Si and O, which is considered the mechanism responsible for material degradation. During this process, the higher content of ATH had a remarkable effect on alleviating surface aging.

INDEX TERMS Moist environment, silicone rubber, hydrophobicity, dry band arc discharge, aging performance.

I. INTRODUCTION

Since the beginning of the power system more than 160 years ago, porcelain and glass have dominated as the selections for outdoor insulator materials because these ceramic insulating materials can generally withstand outdoor stresses. However, in addition to the problems of easy breakdown during transportation, friability, and heavy weight, the pollution-flashover performance of these insulators is poor due to the hydrophilic surface, especially in moist environments with high humidity. During recent decades, therefore, there has been a trend to replace these insulators with polymeric materials [1]–[3]. In particular, silicone rubber (SR) materials with low free surface energy are widely applied because their surface hydrophobicity contributes to superior performance in resisting wetting. Water on the SR surface forms discrete water droplets; therefore, the conductive contaminants dissolved in the water are discontinuous. Another important feature of SR compounds, compared to other polymers, is their ability to recovery from the loss of hydrophobicity. Migration of preexisting low molecular weight (LMW) polydimethylsiloxane (PDMS) fluid from the bulk to the damaged surface are considered as possible mechanisms responsible for the hydrophobic transfer and recovery [4]–[6].

On the other hand, the weak electrostatic bonds between the different atoms in the SR materials result in a polymer insulator that can be degraded more easily than ceramic insulators. The term aging refers to the degradation of an insulator by different environmental effects and electrical stresses. The environmental effects include UV light, heat, moisture, and pollution. Electrical stresses include high electrical field, corona discharge and dry band arc discharge. Surface erosion and tracking that can be generated due to local discharges can destroy hydrophobicity and cause degradation of the

The associate editor coordinating the review of this manuscript and approving it for publication was Mehdi Bagheri.

insulators [7]. Among the above factors, moist environments have a significant impact on the aging performance of SR, especially in coastal regions with high humidity. When the deposited sea salt is diluted in water from drizzle, fog, or light rain, a conductive solution is created, and the leakage current flows on the aged surface. This occurrence will increase the flashover risk of insulators [8].

There has been considerable research effort in the field-aging effects on SR materials of polymer insulators in coastal regions [9]–[13]. The hydrophobicity change varied from the low voltage end to the high voltage end, where the lowest contact angles were found [10]. High leakage current levels were recorded in summer due to high pollution levels and high humidity [12]. Figure 1 shows the peak value of leakage current on an SR insulator on different days in October during field testing on the southern coast of Japan [14]. The leakage current was relatively higher in the early morning and night, while it was lower in the daytime. The condensation water from vapor in moist air at low temperature after sunset was considered the mechanism responsible for the periodic increase in leakage current.

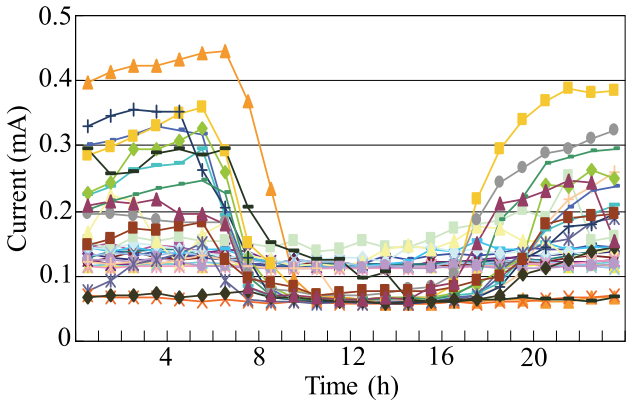

FIGURE 1. Change in leakage current on an SR insulator in a field test.

Testing insulators in a fog chamber have been widely used to study the aging performance of polymer insulators operating in moist environments [15]–[18]. Some studies have focused on leakage current development in the presence of salt-fog and enhanced electric stress. The maximum value of the peak of leakage current and the number of pulses [19]–[21] were reported. The corona from water droplets in the process of loss of hydrophobicity and the development of dry band arcing were also confirmed [22]–[25]. However, the correlation between the discharge development and the surface aging process has not been established clearly, especially the mechanism for hydrophobicity loss and insulation degradation, which still needs to be clarified.

Thus, this study is focused on analyzing the aging mechanism of energized SR exposed to a moist environment. Alumina trihydrate (ATH)-filled high temperature vulcanized (HTV) SR specimens were exposed to a cycling salt-fog test, which simulated the actual dry and humid conditions during the day and night. The development of leakage current and dry band arcing was verified during the test. In addition, physicochemical analyses on the specimens were carried out using scanning electron microscopy (SEM) and X-ray photoelectron spectroscopy (XPS).

II. EXPERIMENTS

A. SINGLE WATER DROPLET TEST

Considering only the discrete water droplets deposited on the hydrophobic SR surface in the initial stage of fog exposure, the behavior of a single water droplet and the induced discharge phenomenon were investigated. The experimental setup is shown in Fig. 2. The homogeneous electric-field gap consisted of two parallel plane electrodes made of stainless steel with one side connected to a high ac-voltage source through a high resistance (15 kΩ) in series and the other side connected to the ground. A plate-shaped HTV SR (including 0% wt%, 30% wt%, 50 wt% and 60% wt% ATH as the filler) of 60 × 50 × 2 mm^3 in size was used as the test specimen, on which a single droplet with a volume of 20 μl (the usual volume of condensation water) and a conductivity of 800 μS/cm (the detected conductivity of seawater) was centrally placed. The electrodes were connected to the specimen by covering the edge of the specimen surface, and the gap between the two electrodes was 20 mm. The applied voltage was raised at a rate of 0.5 kV/s until flashover happened. The leakage current waveform was measured through a 50 Ω resistor in the ground return path. All measured data were displayed on a digital oscilloscope (TDS3000C, Tektronix) and were transferred via a USB bus to a PC for postprocessing. Simultaneously, the behavior of water droplets and discharge phenomena were observed by a high-speed camera (FastcamNet, Photron) at a rate of 1000 frames/s that was triggered by a signal from the oscilloscope.

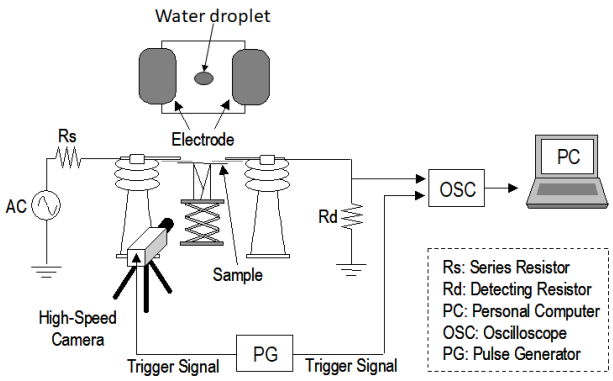

FIGURE 2. Schematic diagram of the experimental setup for the single water droplet test.

B. SALT-FOG TEST

A modified salt-fog test was designed based on IEC 62217. Figure 3 shows a schematic diagram of the salt-fog aging test and leakage current measurement system. The accelerated aging test was conducted in a vinyl chamber (750 × 600 × 600 mm^3), and a supersonic humidifier was

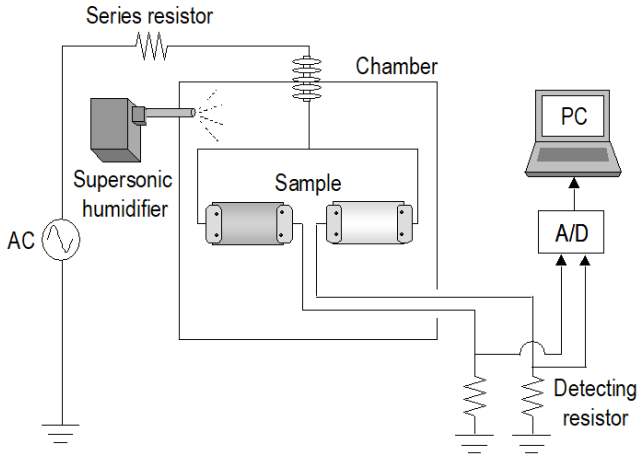

FIGURE 3. Schematic diagram of the experimental setup for the salt-fog aging test.

used to produce a salt-fog with a conductivity of 800 μS/cm at a rate of 0.6 l/h. The homogeneous electric field gap consisted of two parallel plane electrodes made of stainless steel, one side of which was connected to a high ac-voltage source through a high resistance (5 kΩ) in series, whereas the other side was connected to the ground. The plate-shaped HTV SRs (including 0% wt%, 30% wt%, 50 wt% and 60% wt% ATH as the filler) of 80 $\times$ 100 $\times$ 2 mm^3 in size were used as the test specimens. The continually applied voltage was 4.8 kVrms, and the gap length between the two electrodes was 80 mm. An aging cycle comprised two periods, namely, a salt-fog period of 10 h and a dry period of 14 h. The test lasted for 10 cycles for a total of 240 h. The leakage current through a 50 Ω detecting resistor in the ground return path was consecutively acquired and processed by a PC at a rate of 2k samplings/s. Figure 4 shows the specimen surface state during the test. Obvious corona discharge with blue light and arc discharge with orange light can be observed.

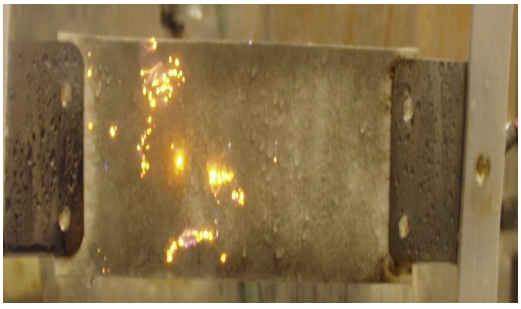

FIGURE 4. Specimen surface state during the salt-fog test.

III. RESULTS AND DISCUSSION

A. EFFECT OF A SINGLE WATER DROPLET

Figure 5 shows the leakage current waveform during 2 s before flashover in the case of the 50 wt% ATH-filled SR specimen. Figure 6 shows the corresponding topical behavior

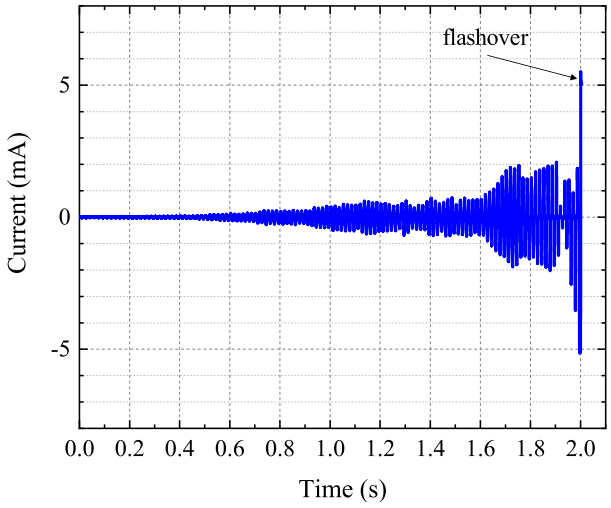

FIGURE 5. Leakage current waveform before flashover in the case of the 50 wt% ATH-filled SR specimen.

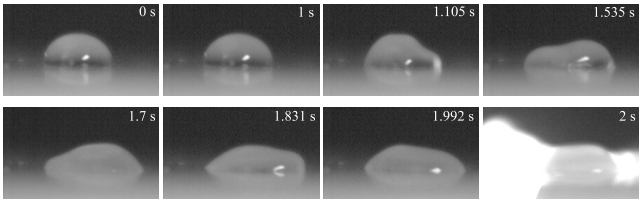

FIGURE 6. Behavior of a water droplet before flashover in the case of the 50 wt% ATH-filled SR specimen.

of the water droplet at certain moments during the same period. The leakage current began to increase at approximately 0.5 s, while there was no obvious change in the shape of the water droplet before 1 s. However, our previous study [23] demonstrated that the calculated electric field was intensified at the triple junction of the water droplet, air and the SR specimen due to the difference in their permittivities, which can ionize the surrounding air and trigger a corona discharge. The corona discharge resulted in an increase in the leakage current at this stage. With the increase in applied voltage after 1 s, the water droplet was polarized and began to vibrate. With a further increase in applied voltage, the water droplet was elongated and expanded to both electrode sides due to the large electrostatic force. The sharp edge of the water droplet tip further enhanced the locally high electric field, and the insulation length between the electrodes was shortened. Meanwhile, the corresponding leakage current significantly increased during this period. Finally, the corona streamer bridged the electrode gap, and flashover happened.

The flashover voltage for the specimens with different ATH contents is shown in Fig. 7. The flashover voltage decreased with increasing ATH content. The surface hydrophobicity is due to the low surface energy of the base PDMS matrix. Thus, the hydrophobicity decreased with increasing inorganic ATH content [11]. The lower contact angle of the water droplet caused a higher local electric field, which is considered the

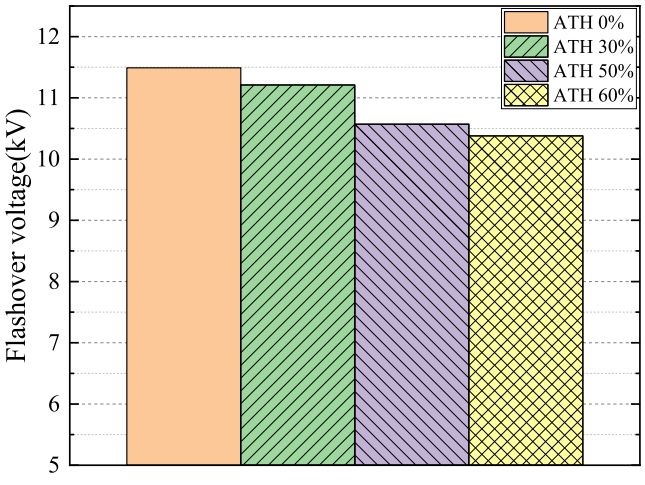

FIGURE 7. Flashover voltage for the specimens with different ATH contents.

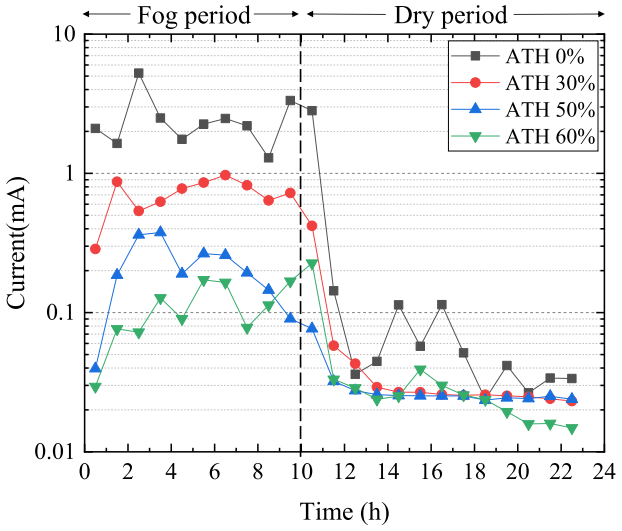

FIGURE 9. Change in leakage current in the last cycle of the salt-fog test.

mechanism responsible for the decay in the flashover voltage of specimens with high ATH content.

B. LEAKAGE CURRENT IN SALT-FOG TEST

During the salt-fog test, the peak value of leakage current per h was recorded, and the results from the first cycle and last cycle are respectively shown in Fig. 8 and Fig. 9. In the same cycle, a higher leakage current in the salt-fog period and a lower leakage current in the dry period can be confirmed, which was consistent with the practical data obtained in the field test shown in Fig. 1. The environment humidity had a significant influence on the leakage current development, and the hydrophobic transfer in the dry period contributed to the surface insulation recovery.

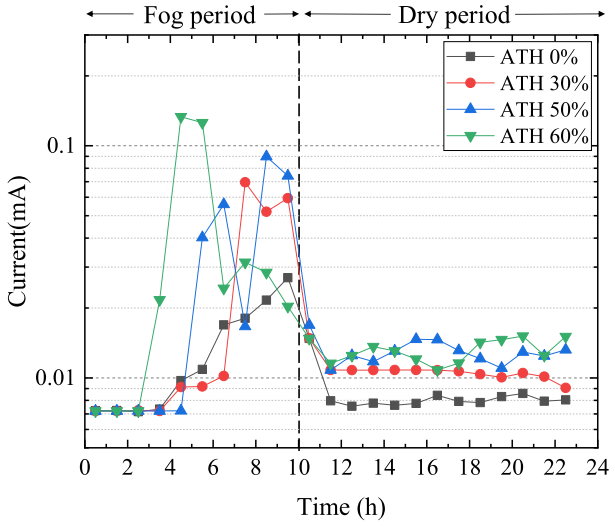

FIGURE 8. Change in leakage current in the first cycle of the salt-fog test.

In the first cycle, the leakage current was very low due to the initially good hydrophobicity. It can also be found that the leakage current increased with increasing ATH content. The relatively higher hydrophobicity of the specimen with a low ATH content than the specimen with a high ATH content had an inhibitory effect on the leakage current development and then formed a relatively higher insulation surface in the initial stage of the salt-fog test. This finding is also confirmed by the results of the single water droplet test.

In the last cycle, the leakage current of all the specimens increased obviously. However, unlike the leakage current characteristics in the first cycle, the leakage current increased with decreasing ATH content. From the observation of the surface state and discharge phenomenon during the whole test, the developing processes can be deduced as several stages. First, discrete water droplets formed on the surface. Next, the corona discharges induced by water droplets gradually degraded the surface hydrophobicity, and then a continuous water channel or water film formed. Thereafter, the specimen lost its ability to suppress the leakage current flow, and then the locally high current density dried the partial water film and formed dry bands. Finally, the majority of the applied voltage was impressed across the dry bands, and if the electric field exceeded the withstand capability, an arc discharge was initiated. The heat from dry band arc discharge became the dominant factor affecting the surface aging, which resulted in possible tracking and erosion and further degraded the surface hydrophobicity. As a flame retardant, ATH has a certain effect on the suppression of thermal aging from dry band arc discharge by the liberation of crystalline water. Thus, the specimen with a higher ATH content has a better inhibitory effect on the leakage current development than the specimen with a lower ATH content, which can be confirmed by the results obtained in the last cycle.

The total cumulative charge and the cumulative dry band arcing charge were evaluated by the separation technique of leakage current reported in [25]. Figure 10 and Figure 11 show the total cumulative charge and the cumulative dry band arcing charge with time, respectively. Both presented an alternate rising trend with the periodic changes between

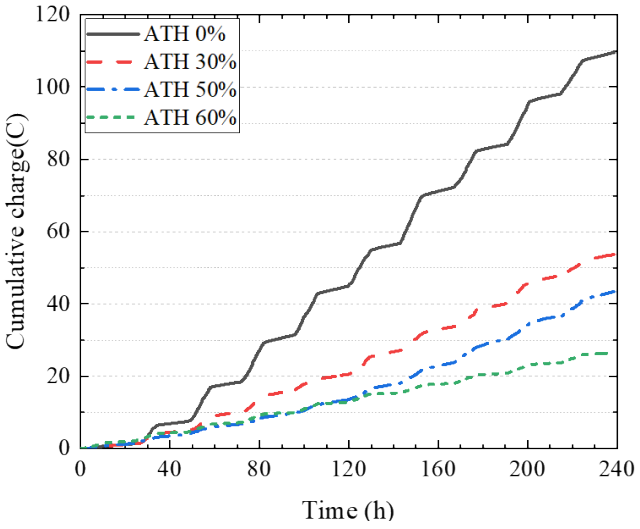

FIGURE 10. Total cumulative charge over time during the salt-fog test.

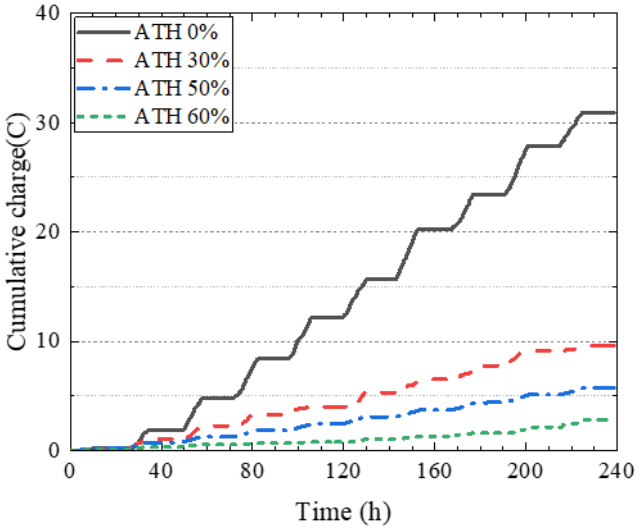

FIGURE 11. Cumulative dry band arcing charge over time during the salt-fog test.

the salt-fog period and dry period. The suppression effect of a higher content of ATH on the development of leakage current and dry band arc discharge was also confirmed.

C. SEM

Figure 12 shows the surface SEM images before and after the salt-fog test in the cases of the 0 wt% and 50 wt% ATH-filled SR specimens. For the unfilled samples, the surface was extremely smooth before test, whereas the surface became pitted, and obvious cracks and erosions occurred after test. For the 50 wt% ATH-filled samples, the fillers were evenly distributed inside the virgin sample, whereas some empty holes were formed after exposure to the dry band arcing in the salt-fog test. This could be caused by the liberation of crystalline water in ATH filler.

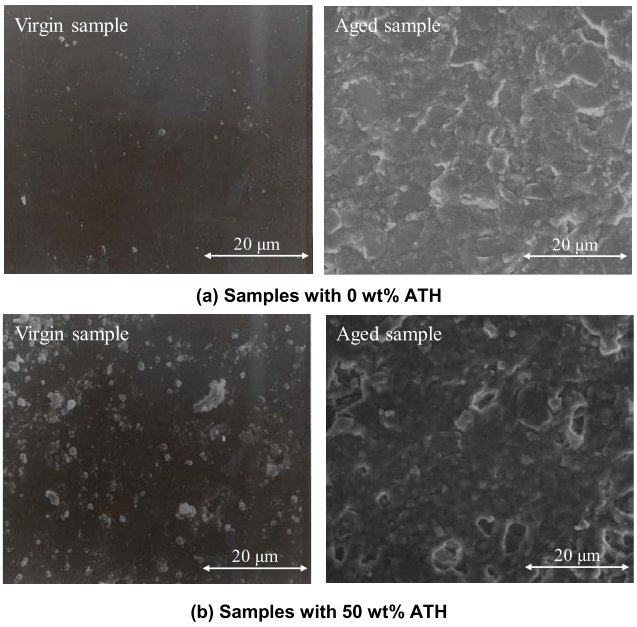

FIGURE 12. SEM images of samples before and after salt-fog test.

D. XPS ANALYSIS

The central region of the specimens was analysed by XPS after the salt-fog test, and the peak separation process was conducted according to the different elementary binding state between Si and O. Figure 13 shows the separated Si 2p photoelectron spectra of aged specimens with different ATH contents and virgin specimens with 0 wt% ATH. Normally, $Si(-O)_1$ 101.5 ± 0.1 eV, $Si(-O)_2$ 102.1 ± 0.1 eV, $Si(-O)_3$ 102.7 ± 0.1 eV and $Si(-O)_4$ 103.4 ± 0.1 eV can be detected in PDMS [26], in which R indicates the CH_3 group. $Si(-O)_2$ is dominant in the chemical structure of virgin specimens, in which the abundant polar CH_3 groups are responsible for the initially good hydrophobicity. However, after the salt-fog test, the proportion of $Si(-O)_2$ was obviously decreased for all the specimens and was replaced by $Si(-O)_3$ and $Si(-O)_4$. The Si–CH_3 side chains in SR were destroyed by the corona discharge and dry band arc discharge during the salt-fog exposure. The decomposition of the Si–CH_3 polar groups is considered the aging mechanism responsible for the hydrophobicity decay in aged SR. Meanwhile, the proportion of $Si(-O)_4$ that had no CH_3 groups decreased with increasing ATH content in the aged specimens. A higher content of ATH has a remarkable effect on alleviating the surface aging and thus suppressing the leakage current development in the salt-fog test, as shown in Figs. 10 and 11.

E. AGING MECHANISM

Figure 14 shows the typical reaction process during the salt-fog test. In the presence of moisture from fog, a hydrolysis reaction might occur in the SR [27]. The heat from the dry band arc discharge can dissociate the side chains of Si–CH_3 as well as dissociate and electrolyze H_2O to -OH and -H. The hydrolysis proceeds to form Si-OH instead of some

① R R—Si—O R	② R O—Si—O R	③ O O—Si—O R	④ O O—Si—O O
$Si(-O)_1$	$Si(-O)_2$	$Si(-O)_3$	$Si(-O)_4$
101.5± 0.1eV	102.1± 0.1 eV	102.7± 0.1eV	103.4± 0.1eV

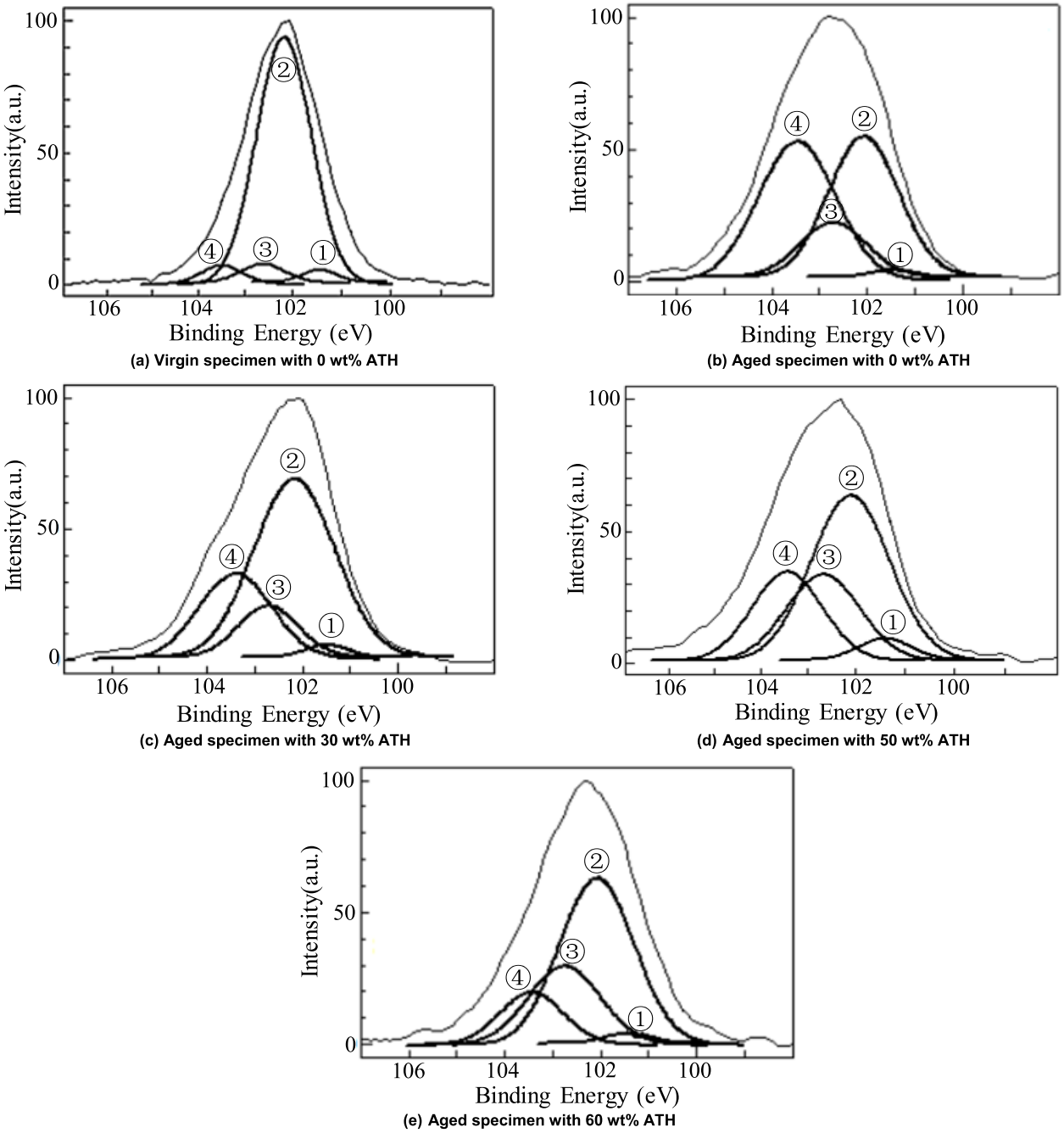

(a) Virgin specimen with 0 wt% ATH

(b) Aged specimen with 0 wt% ATH

(c) Aged specimen with 30 wt% ATH

(d) Aged specimen with 50 wt% ATH

(e) Aged specimen with 60 wt% ATH

FIGURE 13. Si 2p photoelectron spectra of the test specimens.

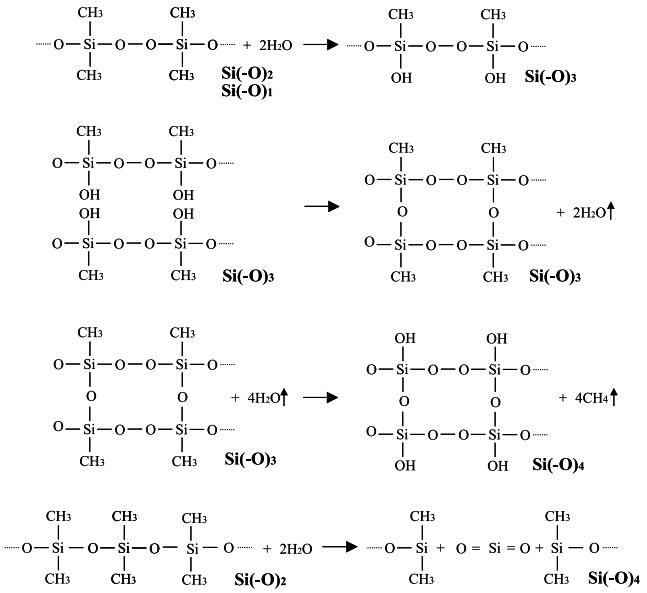

FIGURE 14. Typical reaction process during the salt-fog test.

original hydrophobic Si-CH_3 groups; thus, the binding states of Si(-O)$_1$ and Si(-O)$_2$ change to Si(-O)$_3$. Thereafter, siloxane crosslinking occurs through the dehydration-condensation reaction between the Si-OH groups. Then, during the process of hydrolysis, Si-OH groups replace more Si-CH_3 groups; thus, the binding state of Si(-O)$_4$ forms. In some cases, the heat from dry band arc discharge can directly cause pyrolysis of SR and dissociate the silicone backbone of Si–O–Si to form SiO_2. The abovementioned reaction process can elucidate the mechanism of the change in the binding state between Si and O in the salt-fog test.

IV. CONCLUSION

In this study, the influence of the moist environment on the aging performance of SR used for outdoor insulation was investigated by a cycling salt-fog test. HTV SRs with different ATH filler contents were adopted as the test specimens. For the effect of a single water droplet, the vibration and elongation of the water droplet caused flashover between the electrodes, and the flashover voltage decreased with increasing ATH content. In the salt-fog test, a higher leakage current in the fog period and a lower leakage current in the dry period can be confirmed. In the first cycle, the leakage current increased with increasing ATH content. The relatively higher hydrophobicity of the specimen with a low ATH content than the specimen with a high ATH content had an inhibitory effect on the initial leakage current development. In the last cycle, the heat from dry band arc discharge became the dominant factor for the surface aging after the loss of hydrophobicity, and the specimen with a higher ATH content inversely had a better inhibitory effect on the leakage current development. The changes in the total cumulative charge and the cumulative dry band arcing charge with elapsed time also demonstrated these phenomena. According to the XPS analysis results, when the energized SR was exposed to a moist environment, the heat from dry band arc discharge and the hydrolysis reaction caused the change in the binding state between Si and O, which is considered the mechanism responsible for material degradation. During this process, the higher content of ATH had a remarkable effect on alleviating surface aging and thus suppressed discharge development.

REFERENCES

[1] R. A. Ghunem, S. H. Jayaram, and E. A. Cherney, "Suppression of silicone rubber erosion by alumina trihydrate and silica fillers from dry-band arcing under DC," *IEEE Trans. Dielectrics Electr. Insul.*, vol. 22, no. 1, pp. 14–20, Feb. 2015.

[2] R. Hackam, "Outdoor HV composite polymeric insulators," *IEEE Trans. Dielectr. Electr. Insul.*, vol. 6, no. 5, pp. 557–585, Oct. 1999.

[3] Y. Xue, X.-F. Li, D.-H. Zhang, H.-S. Wang, Y. Chen, and Y.-F. Chen, "Comparison of ATH and SiO_2 fillers filled silicone rubber composites for HTV insulators," *Compos. Sci. Technol.*, vol. 115, pp. 137–143, Feb. 2018.

[4] D. A. Swift, C. Spellman, and A. Haddad, "Hydrophobicity transfer from silicone rubber to adhering pollutants and its effect on insulator performance," *IEEE Trans. Dielectr. Electr. Insul.*, vol. 13, no. 4, pp. 820–829, Aug. 2006.

[5] A. Hergert, J. Kindersberger, C. Bär, and R. Bärsch, "Transfer of hydrophobicity of polymeric insulating materials for high voltage outdoor application," *IEEE Trans. Dielectr. Electr. Insul.*, vol. 24, no. 2, pp. 1057–1067, Apr. 2017.

[6] Y. Zhu, "Influence of corona discharge on hydrophobicity of silicone rubber used for outdoor insulation," *Polym. Test.*, vol. 74, pp. 14–20, Apr. 2019.

[7] M. Amin, M. Akbar, and M. N. Khan, "Aging investigations of polymeric insulators: Overview and bibliography," *IEEE Elect. Insul. Mag.*, vol. 23, no. 4, pp. 44–50, Jul. 2007.

[8] D. Pylarinos, K. Siderakis, and E. Thalassinakis, "Comparative investigation of silicone rubber composite and room temperature vulcanized coated glass insulators installed in coastal overhead transmission lines," *IEEE Elect. Insul. Mag.*, vol. 31, no. 2, pp. 23–29, Mar. 2015.

[9] M. A. R. M. Fernando and S. M. Gubanski, "Ageing of silicone rubber insulators in coastal and inland tropical environment," *IEEE Trans. Dielectr. Electr. Insul.*, vol. 17, no. 2, pp. 326–333, Apr. 2010.

[10] S. M. Rowland, Y. Xiong, J. Robertson, and S. Hoffmann, "Aging of silicone rubber composite insulators on 400 kV transmission lines," *IEEE Trans. Dielectr. Electr. Insul.*, vol. 14, no. 1, pp. 130–136, Feb. 2007.

[11] T. G. Gustavsson, S. M. Gubanski, H. Hillborg, S. Karlsson, and U. W. Gedde, "Aging of silicone rubber under AC or DC voltages in a coastal environment," *IEEE Trans. Dielectr. Electr. Insul.*, vol. 8, no. 6, pp. 1029–1039, Dec. 2001.

[12] A. I. Elombo, J. P. Holtzhausen, H. J. Vermeulen, W. L. Vosloo, and P. J. Pieterse, "Comparative evaluation of the leakage current and aging performance of HTV SR insulators of different creepage lengths when energized by AC, DC+ or DC– in a severe marine environment," *IEEE Trans. Dielectr. Electr. Insul.*, vol. 20, no. 2, pp. 421–428, Apr. 2013.

[13] N. C. Mavrikakis, P. N. Mikropoulos, and K. Siderakis, "Evaluation of field-ageing effects on insulating materials of composite suspension insulators," *IEEE Trans. Dielectr. Electr. Insul.*, vol. 24, no. 1, pp. 409–498, Feb. 2017.

[14] Y. Zhu, H. Yamamoto, M. Otsubo, C. Honda, O. Takenouchi, Y. Hashimoto, and A. Ohno, "On-line monitoring of outdoor polymeric insulators using a novel separation technique of leakage current," in *Proc. 12th Asian Conf. Electr. Discharge*, Shenzhen, China, Nov. 2004, pp. 506–509.

[15] S. Ilhan and E. A. Cherney, "Comparative tests on RTV silicone rubber coated porcelain suspension insulators in a salt-fog chamber," *IEEE Trans. Dielectr. Electr. Insul.*, vol. 25, no. 3, pp. 947–953, Jun. 2018.

[16] X. Jiang, Y. Guo, Z. Meng, Z. Li, and Z. Jiang, "Additional salt deposit density of polluted insulators in salt fog," *IET Gener. Transmiss. Distrib.*, vol. 10, no. 15, pp. 3691–3697, Nov. 2016.

[17] X. Zhangm J. Zhu, S. Bu, Q. Li, V. J. Terzija, and S. M. Rowland, "The development of low-current surface arcs under clean and salt-fog conditions in electricity distribution networks," *IEEE Access*, vol. 6, pp. 15835–15843, 2018.
[18] M. A. Douar, A. Beroual, and X. Souche, "Degradation of various polymeric materials in clean and salt fog conditions: Measurements of AC flashover voltage and assessment of surface damages," *IEEE Trans. Dielectr. Electr. Insul.*, vol. 22, no. 1, pp. 391–399, Feb. 2015.
[19] J. Y. Li, C. X. Sun, and S. A. Sebo, "Humidity and contamination severity impact on the leakage currents of porcelain insulators," *IET Gener., Transmiss. Distrib.*, vol. 5, no. 1, pp. 19–28, Jan. 2011.
[20] R. Ghosh, B. Chatterjee, and S. Chakravorti, "A method for unambiguous identification of on-field recorded insulator leakage current waveforms portraying electrical activity on the surface," *IEEE Trans. Dielectr. Electr. Insul.*, vol. 23, no. 4, pp. 2156–2164, Aug. 2016.
[21] N. A. Othman, M. A. M. Piah, and Z. Adzis, "Space charge distribution and leakage current pulses for contaminated glass insulator strings in power transmission lines," *IET Gener., Transmiss. Distrib.*, vol. 11, no. 4, pp. 876–882, Mar. 2017.
[22] Y. Zhu, K. Haji, M. Otsubo, and C. Honda, "Harmonic analysis of leakage current in salt-fog aging test for polymeric material," *Jpn. J. Appl. Phys.*, vol. 45, no. 11, pp. 8853–8857, Nov. 2006.
[23] Y. Zhu, M. Otsubo, C. Honda, and S. Tanaka, "Corona discharge from water droplet on electrically stressed polymer surface," *Jpn. J. Appl. Phys.*, vol. 45, no. 1A, pp. 234–238, Jan. 2006.
[24] Y. Zhu, M. Otsubo, C. Honda, Y. Hashimoto, and A. Ohno, "Mechanism for change in leakage current waveform on a wet silicone rubber surface-a study using a dynamic 3-D model," *IEEE Trans. Dielectr. Electr. Insul.*, vol. 12, no. 3, pp. 556–565, Jun. 2005.
[25] M. Otsubo, T. Hashiguchi, C. Honda, O. Takenouchi, T. Sakoda, and Y. Hashimoto, "Evaluation of insulation performance of polymeric surface using a novel separation technique of leakage current," *IEEE Trans. Dielectr. Electr. Insul.*, vol. 10, no. 6, pp. 1053–1060, Dec. 2003.
[26] Y. Zhu, K. Haji, M. Otsubo, and C. Honda, "Surface degradation of silicone rubber exposed to corona discharge," *IEEE Trans. Plasma Sci.*, vol. 34, no. 4, pp. 1094–1098, Aug. 2006.
[27] S.-H. Kim, E. A. Cherney, R. Hackam, and K. G. Rutherford, "Chemical changes at the surface of RTV silicone rubber coatings on insulators during dry-band arcing," *IEEE Trans. Dielectr. Electr. Insul.*, vol. 1, no. 1, pp. 106–123, Feb. 1994.

YONG ZHU (M'06) received the B.Eng. degree in electrical engineering from Southeast University, Nanjing, China, in 1998, and the M.Eng. and Ph.D. degrees in electrical engineering from the University of Miyazaki, Miyazaki, Japan, in 2004 and 2007, respectively. From 2007 to 2010, he was a Research Scientist with the High-Voltage Technology Group of Toshiba Corporation, Japan. Since 2010, he has been a Chief Scientist with the Jiangsu Shemar Electric Company, Ltd., China. In 2016, he joined the Department of Electrical Engineering, Taizhou University, China. His research interests include high voltage discharge and polymer insulating materials.

SHENG XU received the B.S. degree in mechanical and electronic engineering from Nanjing Agricultural University, in 1999, the M.S. degree in electrical engineering from the Nanjing University of Science and Technology, in 2005, and the Ph.D. degree in electrical engineering from Southeast University, Nanjing, China, in 2010. In 2011, he joined the Department of Electrical Engineering, Taizhou University, China, where he has been a Professor, since 2018. His current research interests include power quality mitigation and high-voltage equipment.

YANLIN LI received the Ph.D. degree in electrical engineering from the Harbin Institute of Technology, Harbin, China, in 2014. In 2016, he joined the Department of Electrical Engineering, Taizhou University, China, where he has been an Associate Professor, since 2018. His current research interests include microgrid control and high-voltage equipment.